Published in final edited form as:
Neuroscience. 2014 January 31; 258: 90–100. doi:10.1016/j.neuroscience.2013.11.002.

D1-dopamine and α1-adrenergic receptors co-localize in dendrites of the rat prefrontal cortex

Darlene A. Mitrano[a,1], **Jean-Francois Pare**[b], **Yoland Smith**[b], and **David Weinshenker**[a,*]

[a]Department of Human Genetics, Emory University School of Medicine, Atlanta, GA 30322

[b]Department of Neurology and Yerkes National Primate Research Center, Emory University School of Medicine, Atlanta, GA 30322

Abstract

Functional interactions between dopaminergic and noradrenergic systems occur in many brain areas, including the prefrontal cortex (PFC). Biochemical, electrophysiological and behavioral data indicate crosstalk between D1 dopamine receptor (D1R) and α1-adrenergic receptor (α1AR) signaling in the PFC. However, it is unknown whether these interactions occur within the same neurons, or between neurons expressing either receptor. In this study, we used electron microscopy immunocytochemistry to demonstrate that D1Rs and α1ARs co-localize in rat PFC neuronal elements, most prominently in dendrites (60–70%), but also significantly in axon terminals, unmyelinated axons and spines (~20–30%). Our data also showed that the ratio of plasma membrane-bound to intracellular α1ARs is significantly reduced in D1R-expressing dendrites. Similar results were obtained using either a pan-α1AR or a selective α1bAR antibody to label noradrenergic receptors. Thus, these results demonstrate that D1Rs and α1ARs co-localize in PFC dendrites, thereby suggesting that the catecholaminergic effects on PFC function may be driven, at least in part, by cell-autonomous D1R-α1AR interactions.

Keywords

α1-adrenergic receptor; D1 dopamine receptor; prefrontal cortex; electron microscopy; catecholamine

1.1 Catecholaminergic regulation of PFC function

The PFC regulates several executive functions, including working memory, attention, planning, and impulse control (Arnsten and Li, 2005). The neural basis of these functions is of great interest because PFC dysfunction is considered a fundamental feature of several neuropsychiatric disorders, including addiction, attention deficit and hyperactivity disorder

*Address correspondence to David Weinshenker, Ph.D. Department of Human Genetics, Emory University School of Medicine, 615 Michael St., Whitehead 301, Atlanta, GA 30322. Phone: (404) 727-3106, Fax: (404) 727-3949, dweinshenker@genetics.emory.edu.
[1]Current address: Department of Molecular Biology & Chemistry, Christopher Newport University, Newport News, VA 23606

Some of the data in this manuscript have been presented previously in poster form (Society for Neuroscience Annual Meeting).

CONFLICT OF INTEREST
The authors declare no conflicts of interest.

(ADHD), post-traumatic stress disorder (PTSD), and schizophrenia (Goto et al., 2010, Arnsten, 2004, 2007, Hains and Arnsten, 2008).

The catecholamines norepinephrine (NE) (originating from brainstem locus coeruleus neurons) and dopamine (DA) (originating from midbrain ventral tegmental area neurons) are critical for the regulation of PFC activity. For example, catecholamine depletion of the PFC produces deficits in working memory that are as severe as those induced by neuronal lesion in the PFC itself (Brozoski et al., 1979). Furthermore, many of the PFC-associated illnesses listed above are linked to catecholamine dysfunction, and are commonly treated with medications that alter catecholamine transmission (Goto et al., 2010, Gioanni et al., 1998, Arnsten, 2004, 2007, Heal et al., 2009).

1.2 Catecholamine receptors in the PFC

There are several different subtypes of adrenergic and DA receptors. NE signals through α1, α2, and βARs, while DA activates D1-like (D1, D5) and D2-like (D2, D3, D4) receptors. In this study, we focused on the α1-adrenergic receptor (α1AR) and the D1 DA receptor (D1R) because of their importance in PFC function and their noted expression and interactions in this brain region (Weiner et al., 1991, Tassin, 1998, McCune et al., 1993, Pieribone et al., 1994, Gaspar et al., 1995). Of the 3 subtypes of α1ARs (α1a, α1b, α1d), the α1bAR is of particular interest because it is highly expressed in the PFC and is responsible for several α1AR-mediated properties, including regulation of DA transmission (McCune et al., 1993, Pieribone et al., 1994, Drouin et al., 2002).

We have shown previously that α1ARs are most abundant in unmyelinated axons, but are also found in dendrites, spines, and axon terminals in the rat PFC (Mitrano et al., 2012). On the other hand, D1Rs are localized primarily in dendritic spines of pyramidal cells in the PFC of humans and non-human primates (Bergson et al., 1995a, Bergson et al., 1995b), but their subcellular localization in the rodent PFC has not been described.

1.3. D1R-α1AR interactions in the PFC

PFC function is exquisitely sensitive to D1R and α1AR activation. Moderate levels of catecholamines enhance PFC function by activating D1Rs and α2ARs, while high levels of NE and DA impair PFC function by activating α1ARs and overstimulating D1Rs, respectively (Arnsten and Li, 2005, Arnsten, 2007, Hains and Arnsten, 2008). Furthermore, evidence suggests that D1Rs and α1ARs interact with each other in the PFC. For example, ablating dopaminergic innervation of the PFC produces cortical D1R signaling supersensitivity and D1R-mediated locomotor hyperactivity, which can be reversed by either PFC denervation of noradrenergic fibers or intracortical infusion of an α1AR antagonist (Taghzouti et al., 1988, Tassin, 1998). Furthermore, α1AR activation in the PFC facilitates striatal DA transmission and behavioral responses to stimulant drugs like amphetamine, whereas local D1R stimulation in the PFC has the opposite effect (Vezina et al., 1991, Blanc et al., 1994, Darracq et al., 1998, Ventura et al., 2004). D1R-α1AR interactions have also been investigated at the biochemical level in cultured rat PFC neurons, where α1AR activation alters D1R desensitization-resensitization kinetics (Trovero et al., 1994).

Despite these findings, many details concerning D1R-α1AR interactions remain unknown. In this study, we used single and double pre-embedding immunoperoxidase and immunogold methods at the electron microscopic level with antibodies recognizing α1ARs, α1bARs, and D1Rs to determine (1) whether D1R-α1AR interactions can occur within the same neurons expressing both receptor subtypes or likely occur between neurons bearing either of these receptors, (2) the extent of D1R/α1AR colocalization in subcellular and

subsynaptic neuronal compartments, and (3) the specific contribution of the α1bAR subtype to α1AR-D1R co-localization.

2. EXPERIMENTAL PROCEDURES

2.1 Animal treatment for immunocytochemistry

All animal procedures were approved by the Animal Care and Use Committee of Emory University. Eight male, adult Sprague-Dawley rats (200–300 grams) were anesthetized with an overdose of ketamine/medetomidine cocktail before being transcardially perfused with a mixture of paraformaldehyde (4%) and glutaraldehyde (0.1%). Following perfusion, the brains were taken out from the skull, post-fixed in 4% paraformaldehyde overnight, cut in serial 60 um-thick sections with a vibrating microtome and processed with $NaBH_4$ and cryoprotectant in preparation for electron microscopy (EM) immunocytochemistry as described previously (Mitrano and Smith, 2007).

2.2 Primary antibodies for immunocytochemistry

Table 1 describes the primary antibodies and their concentrations used in this study. The specificity of each of these (D1R, α1AR) antibodies has been characterized previously (Ouimet et al., 1984b, Nakadate et al., 2006, Mitrano et al., 2012). The α1bAR antibody was tested by our laboratory in HEK-293 cells and showed labeling in Western Blot analysis only when the cell was transfected with αb1AR DNA. No bands were present when the cells were transfected with mock-DNA or DNA of another receptor (data not shown).

2.3 Single EM pre-embedding immunogold labeling for D1Rs

Sections were pre-incubated for 30 min in PBS containing 5% dry milk at RT (Mitrano and Smith, 2007). They were then incubated in a primary D1R antibody solution overnight at RT, and treated for 2 hr with secondary goat anti-rat IgGs conjugated with 1.4 nm gold particles (1:100; Nanoprobes, Yaphank, NY), followed by silver intensification of gold particles, osmification, dehydration and embedding procedures described previously (Mitrano and Smith, 2007). Omission of the D1R primary antibody resulted in a complete lack of immunogold labeling. Blocks of tissue containing samples of layers V and VI of the medial prefrontal cortex (mPFC) were taken out from the slides, with the aid of rat the brain atlas and previous studies of these brain regions (Vincent et al., 1993, Gaspar et al., 1995, Paxinos and Watson, 1998, Santana et al., 2009) mounted onto resin blocks, and cut into 60-nm sections using an ultramicrotome (Leica Ultracut T2). Layers V and VI of the mPFC were chosen based on results from previous studies (Vincent et al., 1993, Gaspar et al., 1995, Santana et al., 2009) and our pilot light microscopic data (not shown) showing that most D1R labeling is found in these layers in rodents. The 60-nm sections were collected on Pioloform-coated copper grids and examined on a Zeiss EM-10C electron microscope.

In order to examine material in which the antibodies had full access to their antigens, electron microscopic data were collected from superficial ultrathin sections of 3 blocks (from 3 animals) of D1R-immunostained PFC tissue. A total of 50 digital electron micrographs of immunoreactive elements from each block were taken in an unbiased fashion at 31,500X with a CCD camera (DualView 300W; Gatan, Inc., Pleasanton, CA) controlled by DigitalMicrograph software (version 3.10.1, Gatan). Labeled elements (2 gold particles or more for dendrites, axon terminals and glia; 1 gold particle or more for spines and unmyelinated axons) were categorized as dendrites, spines, unmyelinated axons, axon terminals, and glia based on their ultrastructural features (Peters et al., 1991). Spines were usually mushroom-shaped, devoid of mitochondria and displayed a prominent postsynaptic density at asymmetric synapses on their head. Unmyelinated axons were small, circular elements with a relatively smooth and regular shape that traveled straight in the neuropil

when seen in longitudinal plane, often contained tubules, and frequently clustered to form axon bundles. Dendrites were usually round with an irregular contour when cut in the transverse plane. They were highly variable in size depending on their proximity to the parent cell bodies (i.e. large dendrites are more proximal than small dendrites), often contained mitochondria, harbored numerous tubular and pleomorphic organelles, and commonly received synaptic inputs. Glial processes were usually thin, had an irregular morphology, followed a tortuous course to fill space between neuronal elements, and were not found in bundles.

Gold particles were classified as either intracellular (making no contact with the plasma membrane) or plasma membrane-bound (PMB), according to criteria described in detail in our previous study (Mitrano and Smith, 2007). Plasma membrane gold particles were further classified as extrasynaptic (i.e. opposed to the plasma membrane with a distance greater than 20 nm from the nearest synapse); perisynaptic (i.e. either touching the edge of an asymmetric or symmetric synapse or being found less than 20 nm away from the edge of such synapses); or synaptic (i.e. within the body of the postsynaptic specialization of symmetric or asymmetric synapses). Digitally acquired micrographs were adjusted for brightness or contrast using either the DigitalMicrograph or Adobe Photoshop software (version 12.0.4, Adobe Systems Inc.) and then compiled into figures using Adobe Illustrator (version 15.0.2). Statistical analysis and graphs for comparisons of localization of the D1Rs in the various neuronal elements and localization within the element or on the plasma membrane were completed using GraphPad Prism (version 5.04).

2.4 Double EM pre-embedding labeling for D1Rs, α1ARs and α1bARs

In order to determine the extent of co-localization of D1R and α1ARs or α1bARs, we used double pre-embedding immunocytochemistry at the EM level. We first revealed the D1Rs with immunoperoxidase, then the α1ARs with immunogold. To ensure that the percent co-localization obtained from this material was accurate and not dependent on the order in which the different antibodies were localized, we also performed the reverse experiment and labeled the tissue for α1ARs immunoreactivity first with immunoperoxidase, followed by D1Rs with immunogold. Sections were treated as described above and transferred to solutions that contained a mixture of the D1R and α1AR or α1bAR antibodies. To reveal D1Rs immunoreactivity with immunogold, we used secondary goat anti-rat IgGs conjugated with 1.4 nm gold particles (Nanoprobes), while biotinylated goat anti-rat IgGs (1:200, Vector Laboratories, Burlingame, CA) were used when D1Rs were localized with immunoperoxidase. To localize either α1ARs or α1bARs immunoreactivity, goat anti-rabbit IgGs conjugated with 1.4 nm gold particles were used for immunogold, while biotinylated goat anti-rabbit IgGs (1:200, Vector) were used for immunoperoxidase. Silver intensification procedures were performed as described in the preceding section. To reveal immunoperoxidase labeling, sections were incubated, after silver intensification, with the avidin-biotin peroxidase complex (ABC) (1:100; Vector) and then transferred to a 0.025% 3,3-diaminobenzidine tetrahydrochloride (DAB; Sigma St. Louis, MO) solution as described previously (Mitrano & Smith, 2007). Immediately following the DAB reaction, sections were subjected to osmification, dehydration and resin embedding protocol described previously (Mitrano and Smith, 2007). When either primary antibody was paired with both secondary antibodies simultaneously, labeling was indistinguishable from that seen when tissue was incubated with primary and single correct secondary antibody alone (data not shown), indicating that the dual labeling protocol did not impair the labeling of either receptor.

2.5 Additional Control experiments for double pre-embedding labeling

In order to ensure that the secondary antibodies were not sources of any cross-reactions in these double labeling experiments, we paired each primary antibody with the "incorrect" secondary antibody. After $NaBH_4$ treatment, sections were incubated for 1 hour at RT in PBS and 0.3% Triton X-100, followed by one of the primary antibodies listed below. After rinses, sections were incubated in respective secondary biotinylated antibodies at a concentration of 1:200 (Vector). The sections were then run through the ABC and DAB process as described above. Finally, sections were rinsed, mounted onto gelatin-coated slides, dehydrated, and then coverslipped with Permount. The three pairings were as follows: (1) rabbit anti-α1bAR with secondary biotinylated horse anti-mouse IgGs, (2) rabbit anti-α1AR with secondary biotinylated goat anti-rat IgGs, and (3) rat anti-D1R with secondary biotinylated goat anti-rabbit IgGs. Tissue was examined with a Leica DMRB microscope (Leica Microsystems, Inc., Bannockburn, IL, USA) and images were taken at 1X magnification using a CCD camera (Leica DC500), which was controlled by Leica IM50 software. Tissue incubated under each of these 3 conditions did not display any specific immunoreactivity, confirming the specificity of the secondary antibody reactions in our experiments. Representative examples of correctly-paired and incorrectly-paired D1R labeling are shown in Fig. 1.

2.6 Analysis of double pre-embedding labeling

Data were collected from a total of 17 blocks. Four to five animals were used for each data set. All graphs and statistical analysis was performed using GraphPad Prism. Approximately 40 micrographs of randomly selected tissue areas that contained both immunoperoxidase and immunogold labeling in the same field of view were taken from each animal for each receptor combination at 31,500X. From each of these sections, we categorized the ultrastructural features of the different immunoreactive elements labeled with gold, peroxidase or both. In order to assess the specificity and reliability of the gold versus peroxidase staining to label D1Rs and α1ARs, the percentage of double labeled elements was assessed from material in which either receptor subtype was revealed with gold or peroxidase, and vice versa.

For each receptor subtype localized with immunogold, gold particles were categorized as intracellular or plasma membrane-bound using the same criteria as described above for single D1R immunogold labeling above.

3. RESULTS

3.1 Subcellular and subsynaptic localization of D1Rs in the rat PFC

Using immunogold at the electron microscopic level, we found that D1Rs were equally abundant in dendrites and unmyelinated axons (~35–40% each of all labeled elements) in the rat PFC, while expressed at a lower level in spines and axon terminals (~10–15% each) (Fig. 2A). Because glial labeling was almost completely absent, its localization was not quantified. One-way ANOVA revealed a main effect of element ($F_{(3,8)}$=16.61, $p<0.001$). Post hoc tests showed that immunogold labeling was significantly lower in spines ($p<0.01$) and axon terminals ($p<0.05$), but not in unmyelinated axons, compared with dendrites.

There were approximately equal ratios of plasma membrane-bound to intracellular receptor immunoreactivity in spines. A larger fraction of intracellular D1Rs labeling was found in dendrites and axon terminals, while a larger proportion of plasma membrane-bound D1Rs was found in unmyelinated axons (Fig. 2B). Two way ANOVA revealed a main effect of localization ($F_{1,16}$=6.69, $p<0.05$) and localization X element interaction ($F_{3,16}$=9.02, $p<0.01$). Post hoc tests showed that there was significantly less plasma membrane-bound

D1R immunoreactivity compared with intracellular D1R labeling in dendrites and axon terminals. There was a trend for more plasma membrane-bound D1R immunoreactivity compared with intracellular D1R labeling in unmyelinated axons, but the difference did not reach significance. Finally, the majority of D1R plasma membrane labeling was extrasynaptic in dendrites and spines (Fig. 2C), while all axon terminal plasma membrane labeling was extrasynaptic (data not shown). In dendrites, the small amount of labeling that was perisynaptic and synaptic was associated with symmetric synapses, while in spines the perisynaptic and synaptic labeling was associated with asymmetric synapses (Fig. 2C and data not shown). Two way ANOVA revealed a main effect of localization ($F_{2,12}$=73.23, $p<0.0001$) and a localization X element interaction ($F_{2,12}$=5.56, $p<0.05$). Post hoc tests showed that there was a significantly greater proportion of extrasynaptic D1R labeling compared with both perisynaptic and synaptic labeling in both dendrites and spines ($p<0.0001$ for labeling in dendrites; $p<0.01$ for perisynaptic, $p<0.001$ for synaptic labeling in spines). A representative micrograph of D1R labeling is shown in Fig. 2D.

3.2 Co-expression of D1Rs and α1ARs in the PFC

To determine the extent of D1R and α1AR co-expression in the PFC, we labeled D1Rs with immunoperoxidase and α1ARs with immunogold. While only 20–30% of D1-labeled spines, unmyelinated axons, and axon terminals contained α1AR immunogold labeling, as much as 70% of D1R-expressing dendrites co-expressed both receptors (Fig. 3A, B). One-way ANOVA revealed a main effect of element ($F_{3,9}$=5.54, $p<0.05$), and post hoc analysis showed that the co-localization was significantly higher in dendrites compared with other elements. Representative micrographs of D1R (immunoperoxidase) + α1AR (immunogold) double labeling are shown in Fig. 3B. Nearly identical results were obtained when the markers for α1AR and D1Rs were reversed (Fig. 3C, D). One-way ANOVA revealed a main effect of element ($F_{3,12}$=3.83, $p<0.05$), and post hoc analysis showed that co-localization was significantly higher in α1AR-containing dendrites compared with unmyelinated axons and axon terminals. A representative micrograph of D1R (immunogold) + α1AR (immunoperoxidase) double labeling is shown in Fig. 3D.

3.3 Specific pattern of α1AR distribution in D1R-positive dendrites

Because our results indicated that α1ARs and D1Rs show the highest degree of co-expression in dendrites (Fig. 3A, C), and that the subcellular localization of D1R immunoreactivity is significantly different in dendrites than in most other neuronal elements (Fig. 2B), we specifically assessed the subcellular localization of α1AR immunoreactivity in D1R-positive versus D1R-negative dendrites and D1R immunoreactivity in α1AR-positive versus α1AR-negative dendrites. We found that the plasma membrane-bound to intracellular ratio of α1AR labeling was lower in D1R co-expressing dendrites than in dendrites that did not co-express D1Rs (Fig. 4A). A two way ANOVA revealed a main effect of localization ($F_{1,12}$=160.2, $p<0.0001$) and localization X co-expression interaction ($F_{1,12}$=30.78, $p<0.001$). Post hoc analysis showed that the plasma membrane-bound α1AR immunoreactivity was significantly decreased, while intracellular α1AR labeling was significantly increased, in D1R-positive dendrites compared with D1R-negative dendrites (Fig. 4A). By contrast, the subcellular localization of D1R labeling was similar in α1AR-positive and α1AR-negative dendrites (Fig. 4B). Both α1ARs and D1Rs were localized almost exclusively extrasynaptically in both single- and double-labeled elements (data not shown; Mitrano et al., 2012).

3.4 Co-expression of D1Rs and α1bARs in the PFC

To determine whether the α1AR-D1R co-expression and subcellular distribution pattern described using pan α1AR antibodies could be attributed to the α1bAR, we repeated all experiments with an α1bAR-specific antibody, and obtained nearly identical results. The

highest degree of co-expression between D1Rs and α1bAR was in dendrites, whether D1R was revealed with either immunoperoxidase (Fig. 5A; one way ANOVA, $F_{3,16}$=6.37, p<0.01) or immunogold (Fig. 5B; one way ANOVA, $F_{3,9}$=7.02, p<0.01). The ratio of plasma membrane-bound to intracellular α1bARs was lower in D1R co-expressing dendrites than in dendrites that did not co-express D1Rs (Fig. 5C). A two way ANOVA revealed a main effect of localization, ($F_{1,12}$=93, p<0.0001) and localization X co-expression interaction ($F_{1,12}$=4.62, p<0.001). Post hoc analysis showed that the plasma membrane-bound α1bAR immunoreactivity was significantly decreased, while intracellular α1bAR labeling was significantly increased, in D1R-positive dendrites compared with D1R-negative dendrites. By contrast, the dendritic distribution of D1Rs was identical regardless of α1bAR co-expression (Fig. 5D). Nearly all plasma membrane-bound receptors were localized extrasynaptically when examined in single- or double-labeled elements (data not shown). Representative micrograph of D1R and α1bAR double labeling are shown in Fig. 5E and F.

These results suggest that, indeed, α1bAR is the main α1AR subtype detected with the pan α1AR antibodies in the rat PFC.

4. DISCUSSION

4.1 Subcellular distribution of D1Rs in the rat PFC

Studies of D1R expression in the rat and non-human primate PFC by in situ hybridization, receptor autoradiography, and immunocytochemistry indicate that D1Rs are localized in both pyramidal and non-pyramidal neurons (Smiley et al., 1994, Bergson et al., 1995b, Gaspar et al., 1995, Vincent et al., 1995, Davidoff and Benes, 1998, Muly et al., 1998, Goldman-Rakic et al., 2000). However, the ultrastructural localization of D1Rs in the rat medial PFC has not been rigorously assessed. In that regard, our data revealed that D1R immunogold labeling was most abundant in unmyelinated axons and dendrites in layers V and VI of the rat PFC. While this pattern of expression matches data obtained in non-human primates, the subcellular distribution was somewhat different (mostly in axon terminals and spines in monkeys compared with unmyelinated axons and proximal dendrites in rats) (Bordelon-Glausier et al., 2008). This discrepancy could be explained by the differential organization of the cortex in rodents versus monkeys. In addition, our electron microscopic analysis was performed in blocks of tissue from deep cortical layers where spines are rare compared with dendrites, terminals, and cell bodies, while some of the non-human primate studies were focused on more superficial layers of the PFC (Bergson et al., 1995b). However, D1Rs were also found predominantly on spines in deeper layers of the non-human primate PFC (Bordelon-Glausier et al., 2008), suggesting the existence of a true species difference in D1R localization. We also found that while there is roughly an equal proportion of D1R labeling associated with the plasma membrane and the intracellular compartment of spines, dendrites expressed a significantly larger proportion of intracellular labeling, suggesting that the labeling may be associated with actively trafficking receptors in dendritic structures, although recent evidence indicates that these intracellular receptors may also be capable of signaling (Calebiro et al., 2010).

4.2 Colocalization of D1Rs and α1ARs in the PFC

There are many aspects of PFC function that are differently affected by D1R and α1AR signaling, although the mechanisms underlying these, often opposite, properties remain poorly understood. For instance, moderate activation of D1Rs can improve working memory, while α1AR activation impairs it (Arnsten and Li, 2005, Arnsten, 2007, Hains and Arnsten, 2008). Blockade of α1ARs in the PFC attenuates mesolimbic DA transmission and psychostimulant behavioral sensitization, whereas intra-PFC antagonism of D1Rs facilitates

sensitization (Vezina et al., 1991, Darracq et al., 1998, Ventura et al., 2004). There is also evidence that D1R and α1AR signaling pathways interact in a more direct manner. Electrolytic VTA lesions produce a compensatory upregulation of D1R signaling in the PFC and locomotor hyperactivity that are both abolished by α1AR blockade (Taghzouti et al., 1988, Trovero et al., 1992, Tassin, 1998). The best evidence for a direct interaction between D1R and α1AR function was a study that utilized cultured PFC and striatal neurons. The investigators found that the resensitization of D1Rs following desensitization induced by chronic DA exposure was accelerated by an α1AR agonist only in PFC neurons, but by glutamate in striatal neurons (Trovero et al., 1994). Our data indicate that a majority (~70%) of D1R-expressing dendrites in the PFC also expresses α1ARs, and vice versa, a substrate through which functional interactions between these receptors could occur at the single neuron level. By contrast, while D1R expression is also high in dendrites of striatal medium spiny neurons, we have shown previously that α1AR expression is almost entirely restricted to axons and axon terminals in this brain region (Mitrano and Smith, 2007, Rommelfanger et al., 2009). These results indicate minimal co-expression of D1Rs and α1ARs in striatal dendrites and are consistent with the reported PFC-specific biochemical interaction described above (Trovero et al., 1994).

Co-expression in other neuronal elements was modest (~20–30%), suggesting that robust receptor-receptor interactions may be restricted to the dendritic compartments in PFC. Although our study did not directly address the potential functional significance of high dendritic co-localization compared with other elements, it may reflect faster access by downstream receptor signaling molecules to dendritic ribosomes for control of local protein translation and to the nucleus for control of gene expression.

We also found that the subcellular localization of α1ARs and D1Rs in dendrites of layers V and VI PFC neurons differed from other elements. While approximately half of the labeling for either receptor subtype was localized to the plasma membrane in most neuronal elements examined, dendrites exhibited a much higher level of intracellular than plasma membrane-bound immunoreactivity. Furthermore, this higher proportion of intracellular labeling for α1ARs was significantly more pronounced in D1R-containing dendrites compared with D1R-negative dendrites, raising the possibility that the presence of D1Rs directly or indirectly alters the plasma membrane trafficking of α1ARs in layer V/VI PFC neurons. Because D1Rs and α1ARs can internalize in response to agonist exposure (Ng et al., 1995, Chalothorn et al., 2002), the large proportion of intracellular α1AR labeling may reflect a higher rate of receptor internalization or receptor trafficking in D1R-positive dendrites. While internalization is classically thought to attenuate signaling, recent evidence indicates that internalized receptors retain signaling capacity (Vincent et al., 1995, Calebiro et al., 2010). Certain combinations of adrenergic and DA receptor subtypes are capable of heterodimerization, and agonist-induced cross-internalization of linked GPCRs can occur (Prinster et al., 2005, Gonzalez et al., 2012, Rebois et al., 2012). Future experiments are required to determine whether α1ARs and D1Rs can heterodimerize and affect each other's trafficking in PFC neurons. It is important to keep in mind that these experiments represent single "snapshots" of the receptors in experimentally naïve rats. Further studies utilizing pharmacological (e.g. receptor agonist or psychostimulant administration) and environmental (e.g. stress) manipulations will be required to generate a more complete picture of D1R and α1AR co-expression and distribution.

Although our data were obtained using pan α1AR antibodies that recognize all three α1AR subtypes (a, b, and d), the fact that similar patterns of labeling and co-localization with D1Rs were obtained with specific α1bAR antibodies suggest that this particular subtype of α1AR may be preferentially involved in these interactions with the D1R, although the

distribution of α1aARs and α1dARs must also be studied in greater detail to determine the degree of specificity of these interactions.

4.3 Implications for the contribution of catecholamine transmission in the PFC to working memory and neuropsychiatric disorders

The results presented here have important implications for PFC function in normal and diseased states. As mentioned in the Introduction, working memory is under tight control of catecholamine signaling in the PFC. In general, activation of D1Rs and α2ARs in the PFC facilitates working memory, while activation of α1ARs impairs these processes (Arnsten and Li, 2005, Arnsten, 2007, Hains and Arnsten, 2008, Zhang et al., 2013). Our finding that D1Rs and α1ARs reside together in PFC dendrites provides a potential neuroanatomical substrate for some opposing actions of these receptors. Catecholaminergic drugs are also first-line treatments for neuropsychiatric disorders such as ADHD, and accumulating evidence suggests that the PFC is a critical neuroanatomical substrate for their beneficial effects. For example, methylphenidate, which increases extracellular DA and NE levels, facilitates working memory and improves PFC function via activation of both dopaminergic and adrenergic receptors when infused directly into the PFC (Heal et al., 2009, Seong & Carter, 2012). Interestingly, the ability of methylphenidate to augment sustained attention and attentional set-shifting was blocked by an α1AR antagonist, suggesting that α1AR activation can also have beneficial effects on PFC function (Berridge et al., 2012). The data presented here indicate that the effects of these therapeutic drugs may be mediated, at least in part, by direct D1R-α1AR interactions in PFC pyramidal cell dendrites.

PFC dysfunction has been implicated in drug addiction, and D1R and α1AR signaling in this structure is critical for behavioral and neurochemical responses to psychostimulants. Notably, α1AR activation in the PFC facilitates psychostimulant-induced locomotor activity, sensitization, and DA release in the nucleus accumbens (Blanc et al., 1994, Darracq et al., 1998), while activation of D1Rs in the PFC tends to have the opposite effects (Vezina et al., 1991). In contrast to its facilitatory effects on drug-induced motor activity, D1R blockade in the PFC actually prevents several forms of drug-seeking behavior (Capriles et al., 2003, Sun & Rebec, 2005), an effect shared by α1AR blockade in the PFC (our unpublished data). D1R-α1AR interactions in PFC neurons may underlie some of these complex effects receptor signaling in the PFC on behaviors relevant to drug addiction.

4.4. Conclusions

Our findings demonstrate that D1Rs and α1ARs co-localize to multiple subcellular compartments in the rat PFC, the distribution of α1ARs is altered in D1-expressing dendrites, and the patterns are similar using a pan-α1AR antibody or one selective for the α1bAR subtype. These results have implications for catecholaminergic control of normal PFC function, as well as dysfunction in disease states.

Acknowledgments

This work was supported by the National Institute of Drug Abuse (DA027535 to DW), the National Institute of General Medical Sciences (5K12GM000680 to DAM) and the NCRR base grant of the Yerkes National Primate Research Center (RR00165).

Bibliography

Arnsten AF. Adrenergic targets for the treatment of cognitive deficits in schizophrenia. Psychopharmacology (Berl). 2004; 174:25–31. [PubMed: 15205875]

Arnsten AF. Catecholamine and second messenger influences on prefrontal cortical networks of "representational knowledge": a rational bridge between genetics and the symptoms of mental illness. Cereb Cortex. 2007; 17(Suppl 1):i6–15. [PubMed: 17434919]

Arnsten AF, Li BM. Neurobiology of executive functions: catecholamine influences on prefrontal cortical functions. Biol Psychiatry. 2005; 57:1377–1384. [PubMed: 15950011]

Bergson C, Mrzljak L, Lidow MS, Goldman-Rakic PS, Levenson R. Characterization of subtype-specific antibodies to the human D5 dopamine receptor: studies in primate brain and transfected mammalian cells. Proc Natl Acad Sci U S A. 1995a; 92:3468–3472. [PubMed: 7536933]

Bergson C, Mrzljak L, Smiley JF, Pappy M, Levenson R, Goldman-Rakic PS. Regional, cellular, and subcellular variations in the distribution of D1 and D5 dopamine receptors in primate brain. J Neurosci. 1995b; 15:7821–7836. [PubMed: 8613722]

Berridge CW, Berridge CW, Shumsky JS, Andrzejewski ME, McGaughy JA, Spencer RC, Devilbiss DM, Waterhouse BD. Differential sensitivity to psychostimulants across prefrontal cognitive tasks: differential involvement of noradrenergic α- and α-receptors. Biol Psychiatry. 2012; 71:467–473. [PubMed: 21890109]

Blanc G, Trovero F, Vezina P, Herve D, Godeheu AM, Glowinski J, Tassin JP. Blockade of prefronto-cortical alpha 1-adrenergic receptors prevents locomotor hyperactivity induced by subcortical D-amphetamine injection. Eur J Neurosci. 1994; 6:293–298. [PubMed: 7912614]

Bordelon-Glausier JR, Khan ZU, Muly EC. Quantification of D1 and D5 dopamine receptor localization in layers I, III, and V of Macaca mulatta prefrontal cortical area 9: coexpression in dendritic spines and axon terminals. J Comp Neurol. 2008; 508:893–905. [PubMed: 18399540]

Brozoski TJ, Brown RM, Rosvold HE, Goldman PS. Cognitive deficit caused by regional depletion of dopamine in prefrontal cortex of rhesus monkey. Science. 1979; 205:929–932. [PubMed: 112679]

Calebiro D, Nikolaev VO, Persani L, Lohse MJ. Signaling by internalized G-protein-coupled receptors. Trends Pharmacol Sci. 2010; 31:221–228. [PubMed: 20303186]

Capriles N, Rodaros D, Sorge RE, Stewart J. A role for the prefrontal cortex in stress- and cocaine-induced reinstatement of cocaine seeking in rats. Psychopharmacology (Berl). 2003; 168:66–74. [PubMed: 12442201]

Chalothorn D, McCune DF, Edelmann SE, Garcia-Cazarin ML, Tsujimoto G, Piascik MT. Differences in the cellular localization and agonist-mediated internalization properties of the alpha(1)-adrenoceptor subtypes. Mol Pharmacol. 2002; 61:1008–1016. [PubMed: 11961118]

Darracq L, Blanc G, Glowinski J, Tassin JP. Importance of the noradrenaline-dopamine coupling in the locomotor activating effects of D-amphetamine. J Neurosci. 1998; 18:2729–2739. [PubMed: 9502830]

Davidoff SA, Benes FM. High-resolution scatchard analysis shows D1 receptor binding on pyramidal and nonpyramidal neurons. Synapse. 1998; 28:83–90. [PubMed: 9414021]

Drouin C, Darracq L, Trovero F, Blanc G, Glowinski J, Cotecchia S, Tassin JP. Alpha1b-adrenergic receptors control locomotor and rewarding effects of psychostimulants and opiates. J Neurosci. 2002; 22:2873–2884. [PubMed: 11923452]

Gaspar P, Bloch B, Le Moine C. D1 and D2 receptor gene expression in the rat frontal cortex: cellular localization in different classes of efferent neurons. Eur J Neurosci. 1995; 7:1050–1063. [PubMed: 7613610]

Gioanni Y, Thierry AM, Glowinski J, Tassin JP. Alpha1-adrenergic, D1, and D2 receptors interactions in the prefrontal cortex: implications for the modality of action of different types of neuroleptics. Synapse. 1998; 30:362–370. [PubMed: 9826228]

Goldman-Rakic PS, Muly EC 3rd, Williams GV. D(1) receptors in prefrontal cells and circuits. Brain Res Brain Res Rev. 2000; 31:295–301. [PubMed: 10719156]

Gonzalez S, Moreno-Delgado D, Moreno E, Perez-Capote K, Franco R, Mallol J, Cortes A, Casado V, Lluis C, Ortiz J, Ferre S, Canela E, McCormick PJ. Circadian-related heteromerization of adrenergic and dopamine D(4) receptors modulates melatonin synthesis and release in the pineal gland. PLoS Biol. 2012; 10:e1001347. [PubMed: 22723743]

Goto Y, Yang CR, Otani S. Functional and dysfunctional synaptic plasticity in prefrontal cortex: roles in psychiatric disorders. Biol Psychiatry. 2010; 67:199–207. [PubMed: 19833323]

Hains AB, Arnsten AF. Molecular mechanisms of stress-induced prefrontal cortical impairment: implications for mental illness. Learn Mem. 2008; 15:551–564. [PubMed: 18685145]

Heal DJ, Cheetham SC, Smith SL. The neuropharmacology of ADHD drugs in vivo: insights on efficacy and safety. Neuropharmacology. 2009; 57:608–618. [PubMed: 19761781]

McCune SK, Voigt MM, Hill JM. Expression of multiple alpha adrenergic receptor subtype messenger RNAs in the adult rat brain. Neuroscience. 1993; 57:143–151. [PubMed: 8278048]

Mitrano DA, Schroeder JP, Smith Y, Cortright JJ, Bubula N, Vezina P, Weinshenker D. Alpha-1 Adrenergic Receptors are Localized on Presynaptic Elements in the Nucleus Accumbens and Regulate Mesolimbic Dopamine Transmission. Neuropsychopharmacology. 2012; 37:2161–2172. [PubMed: 22588352]

Mitrano DA, Smith Y. Comparative analysis of the subcellular and subsynaptic localization of mGluR1a and mGluR5 metabotropic glutamate receptors in the shell and core of the nucleus accumbens in rat and monkey. J Comp Neurol. 2007; 500:788–806. [PubMed: 17154259]

Muly EC 3rd, Szigeti K, Goldman-Rakic PS. D1 receptor in interneurons of macaque prefrontal cortex: distribution and subcellular localization. J Neurosci. 1998; 18:10553–10565. [PubMed: 9852592]

Nakadate K, Imamura K, Watanabe Y. Cellular and subcellular localization of alpha-1 adrenoceptors in the rat visual cortex. Neuroscience. 2006; 141:1783–1792. [PubMed: 16797131]

Ng GY, Trogadis J, Stevens J, Bouvier M, O'Dowd BF, George SR. Agonist-induced desensitization of dopamine D1 receptor-stimulated adenylyl cyclase activity is temporally and biochemically separated from D1 receptor internalization. Proc Natl Acad Sci U S A. 1995; 92:10157–10161. [PubMed: 7479745]

Ouimet CC, Miller PE, Hemmings HC Jr, Walaas SI, Greengard P. DARPP-32, a dopamine- and adenosine 3′:5′-monophosphate-regulated phosphoprotein enriched in dopamine-innervated brain regions. III. Immunocytochemical localization. J Neurosci. 1984; 4:111–124. [PubMed: 6319625]

Paxinos, G.; Watson, C. The Rat Brain In Stereotaxic Coordinates. London: Academic Press Limited; 1998.

Peters, A.; Palay, S.; Webster, HD. The fine structure of the nervous system: Neurons and their supporting cells. Oxford University Press; New York: 1991.

Pieribone VA, Nicholas AP, Dagerlind A, Hokfelt T. Distribution of alpha 1 adrenoceptors in rat brain revealed by in situ hybridization experiments utilizing subtype-specific probes. J Neurosci. 1994; 14:4252–4268. [PubMed: 8027777]

Prinster SC, Hague C, Hall RA. Heterodimerization of g protein-coupled receptors: specificity and functional significance. Pharmacol Rev. 2005; 57:289–298. [PubMed: 16109836]

Rebois RV, Maki K, Meeks JA, Fishman PH, Hebert TE, Northup JK. D2-like dopamine and beta-adrenergic receptors form a signaling complex that integrates Gs- and Gi-mediated regulation of adenylyl cyclase. Cell Signal. 2012; 24:2051–2060. [PubMed: 22759790]

Rommelfanger KS, Mitrano DA, Smith Y, Weinshenker D. Light and electron microscopic localization of alpha-1 adrenergic receptor immunoreactivity in the rat striatum and ventral midbrain. Neuroscience. 2009; 158:1530–1540. [PubMed: 19068224]

Santana N, Mengod G, Artigas F. Quantitative analysis of the expression of dopamine D1 and D2 receptors in pyramidal and GABAergic neurons of the rat prefrontal cortex. Cereb Cortex. 2009; 19:849–860. [PubMed: 18689859]

Seong HJ, Carter AG. D1 receptor modulation of action potential firing in a subpopulation of layer 5 pyramidal neurons in the prefrontal cortex. J Neurosci. 2012; 32:10516–10521. [PubMed: 22855801]

Smiley JF, Levey AI, Ciliax BJ, Goldman-Rakic PS. D1 dopamine receptor immunoreactivity in human and monkey cerebral cortex: predominant and extrasynaptic localization in dendritic spines. Proc Natl Acad Sci U S A. 1994; 91:5720–5724. [PubMed: 7911245]

Sun W, Rebec GV. The role of prefrontal cortex D1-like and D2-like receptors in cocaine-seeking behavior in rats. Psychopharmacology (Berl). 2005; 177:315–23. [PubMed: 15309375]

Taghzouti K, Simon H, Hervé D, Blanc G, Studler JM, Glowinski J, LeMoal M, Tassin JP. Behavioural deficits induced by an electrolytic lesion of the rat ventral mesencephalic tegmentum

are corrected by a superimposed lesion of the dorsal noradrenergic system. Brain Res. 1988; 440:172–176. [PubMed: 3129124]

Tassin JP. Norepinephrine-dopamine interactions in the prefrontal cortex and the ventral tegmental area: relevance to mental diseases. Adv Pharmacol. 1998; 42:712–716. [PubMed: 9327998]

Trovero F, Blanc G, Hervé D, Vézina P, Glowinski J, Tassin JP. Contribution of an alpha 1-adrenergic receptor subtype to the expression of the “ventral tegmental area syndrome”. Neuroscience. 1992; 47:69–76. [PubMed: 1349733]

Trovero F, Marin P, Tassin JP, Premont J, Glowinski J. Accelerated resensitization of the D1 dopamine receptor-mediated response in cultured cortical and striatal neurons from the rat: respective role of alpha 1-adrenergic and N-methyl-D-aspartate receptors. J Neurosci. 1994; 14:6280–6288. [PubMed: 7931580]

Ventura R, Alcaro A, Cabib S, Conversi D, Mandolesi L, Puglisi-Allegra S. Dopamine in the medial prefrontal cortex controls genotype-dependent effects of amphetamine on mesoaccumbens dopamine release and locomotion. Neuropsychopharmacology. 2004; 29:72–80. [PubMed: 12968132]

Vezina P, Blanc G, Glowinski J, Tassin JP. Opposed Behavioural Outputs of Increased Dopamine Transmission in Prefrontocortical and Subcortical Areas: A Role for the Cortical D-1 Dopamine Receptor. Eur J Neurosci. 1991; 3:1001–1007. [PubMed: 12106258]

Vincent SL, Khan Y, Benes FM. Cellular distribution of dopamine D1 and D2 receptors in rat medial prefrontal cortex. J Neurosci. 1993; 13:2551–2564. [PubMed: 8501521]

Vincent SL, Khan Y, Benes FM. Cellular colocalization of dopamine D1 and D2 receptors in rat medial prefrontal cortex. Synapse. 1995; 19:112–120. [PubMed: 7725240]

Weiner DM, Levey AI, Sunahara RK, Niznik HB, O’Dowd BF, Seeman P, Brann MR. D1 and D2 dopamine receptor mRNA in rat brain. Proc Natl Acad Sci U S A. 1991; 88:1859–1863. [PubMed: 1825729]

Zhang Z, Cordeiro Matos S, Jego S, Adamantidis A, Seguela P. Norepinephrine Drives Persistent Activity in Prefrontal Cortex via Synergistic alpha1 and alpha2 Adrenoceptors. PloS One. 2013; 8:e66122. [PubMed: 23785477]

Highlights

- D1 dopamine and α1-adrenergic receptors co-localize in prefrontal cortex neurons
- Amount of co-localization is greatest in dendrites
- A greater fraction of α1 receptors are intracellular in D1 co-expressing dendrites
- Identical results were found for the α1b subtype

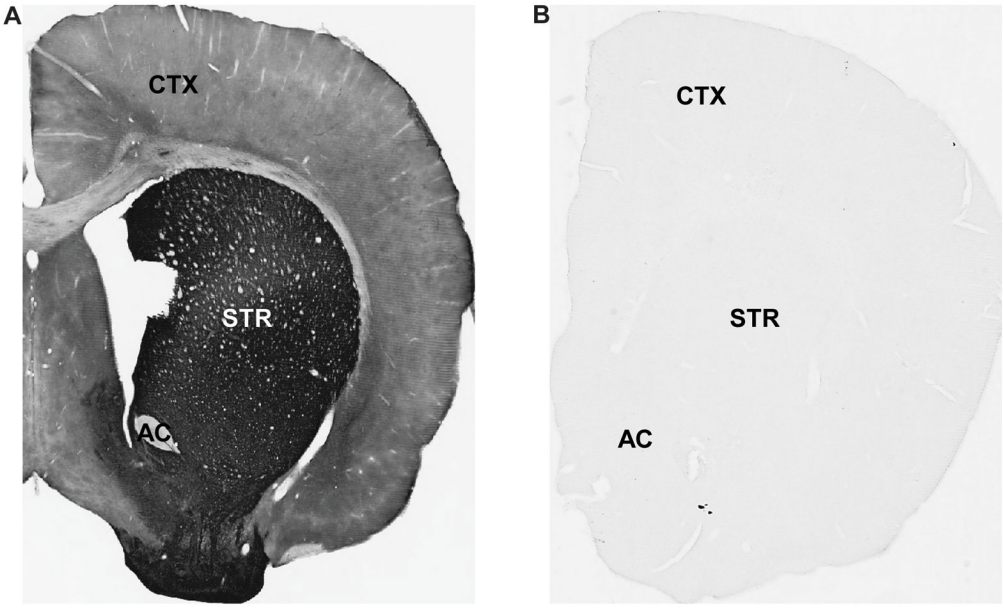

Fig. 1. Control experiments for double pre-embedding labeling

(A) Representative example of D1R immunoreactivity when primary antibody was paired with the correct secondary antibody. (B) Representative example of the lack of D1R immunoreactivity when primary antibody was paired with the incorrect secondary antibody. AC=anterior commissure; STR=striatum; CTX=cortex. Magnification=1X.

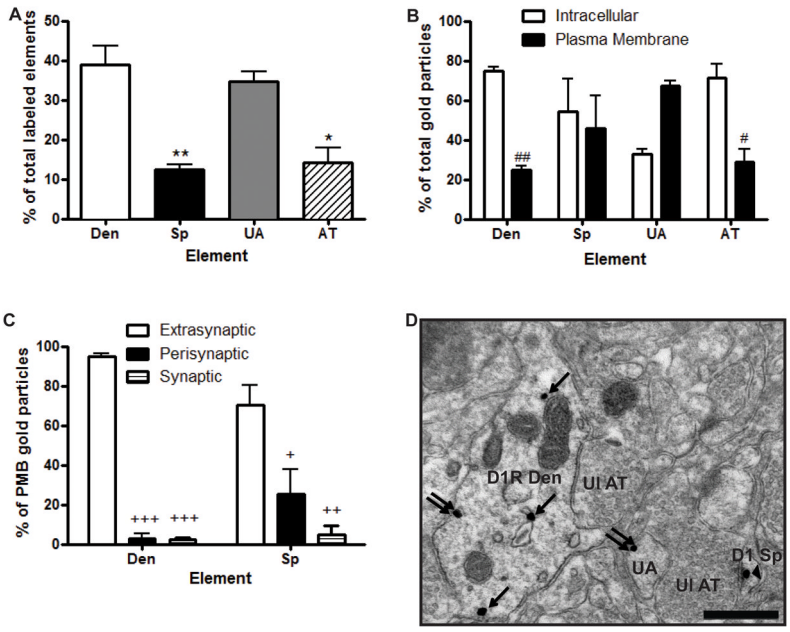

Fig. 2. Ultrastructural and subsynaptic localization of D1Rs in the PFC

(A) Mean ± SEM percent of total D1R-labeled neuronal elements in the PFC as revealed with the pre-embedding immunogold method. *p<0.05, **p<0.01 compared to dendrites. (B) Mean ± SEM percent total D1R immunogold particle labeling associated with the plasma membrane or the intracellular compartment in different PFC neuronal elements. #p<0.05, ##p<0.01 compared to intracellular compartment for that element. (C) Mean ± SEM percent of D1Rs localization on dendrites and spines when associated with the plasma membrane. +p<0.01, ++ p<0.001, +++p<0.0001 compared to extrasynaptic labeling for that element. (D) Representative electron micrograph of a D1R-labeled dendrite, unmyelinated axon and spine. Single arrows indicate intracellular gold particles, double arrows indicate plasma membrane bound extrasynaptic labeling, and arrowhead indicates synaptic labeling at an asymmetric synapse. N=3 rats. Total number of labeled elements examined: 132 dendrites, 42 spines, 120 unmyelinated axons, and 50 axon terminals. Total number of immunogold particles counted: 470 from dendrites, 83 from spines, 255 from unmyelinated axons, and 142 from axon terminals. Den, dendrite; Sp, dendritic spine; UA, unmyelinated axon; AT, axon terminal; Ul, unlabeled. Scale bar = 0.5 μm.

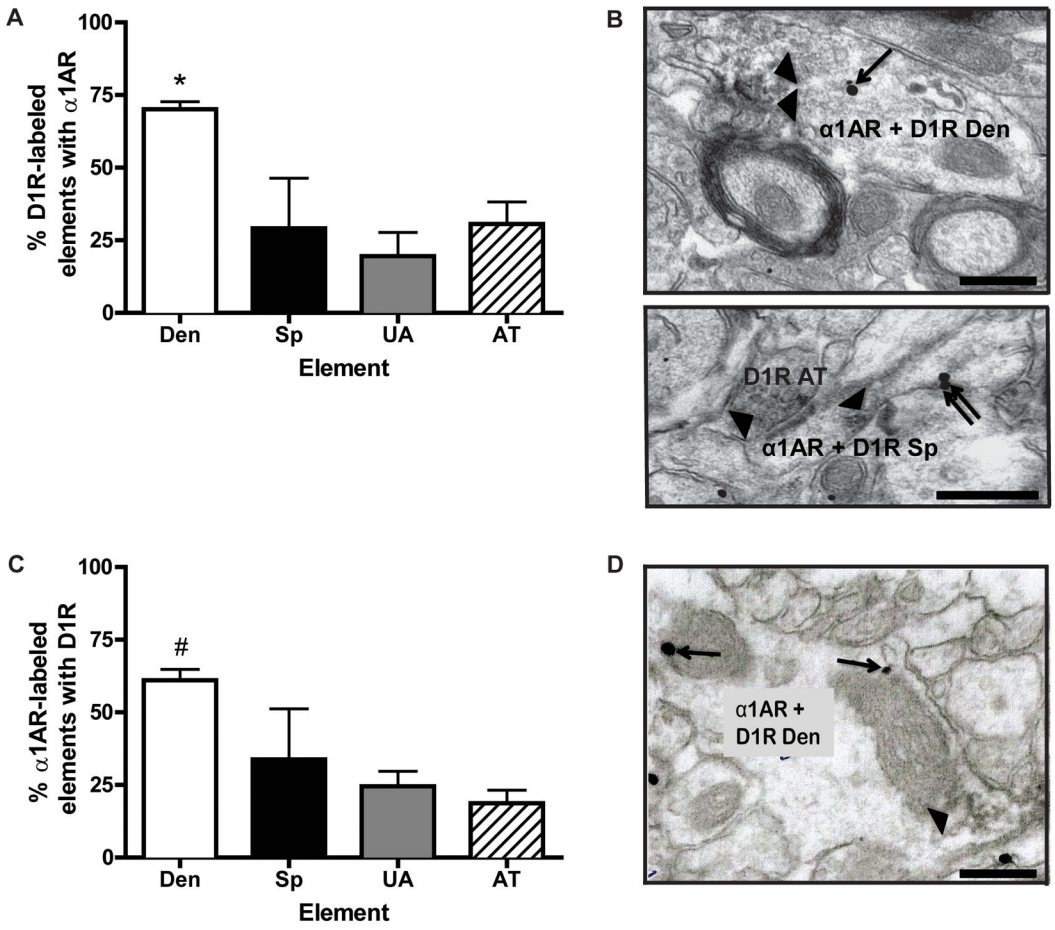

Fig. 3. D1R and α1AR co-localization in the PFC

(A) Mean ± SEM percent of D1R immunoperoxidase-labeled elements that also contain α1AR immunogold labeling. Each bar represents the relative percentage of different categories of D1R-positive elements that co-express α1AR immunoreactivity. N=4 rats. Total number of D1R-labeled elements examined: 89 dendrites, 17 spines, 61 unmyelinated axons, and 18 axon terminals. *$p<0.05$ compared with other neuronal elements. (B) Top, representative electron micrograph of a double labeled dendrite for D1R (immunoperoxidase) and α1AR (immunogold) immunoreactivity; bottom, a double labeled spine synapsing on a D1R-positive axon terminal. (C) Mean ± SEM percent of α1AR immunoperoxidase-labeled elements that also contain D1R immunogold labeling. N=4 rats. Total number of α1AR-labeled elements examined: 147 dendrites, 27 spines, 259 unmyelinated axons, and 76 axon terminals. #$p<0.05$ compared with other elements, except for spines. (D) Representative electron micrograph of a double labeled dendrite for α1AR (immunoperoxidase labeling) and D1R (immunogold labeling). Single arrows indicate intracellular labeling, double arrows indicate extrasynaptic plasma membrane labeling, and arrowheads indicate areas of diffuse immunoperoxidase labeling. Den, dendrite; Sp, dendritic spine; UA, unmyelinated axon; AT, axon terminal. Scale bars = 0.5 μm.

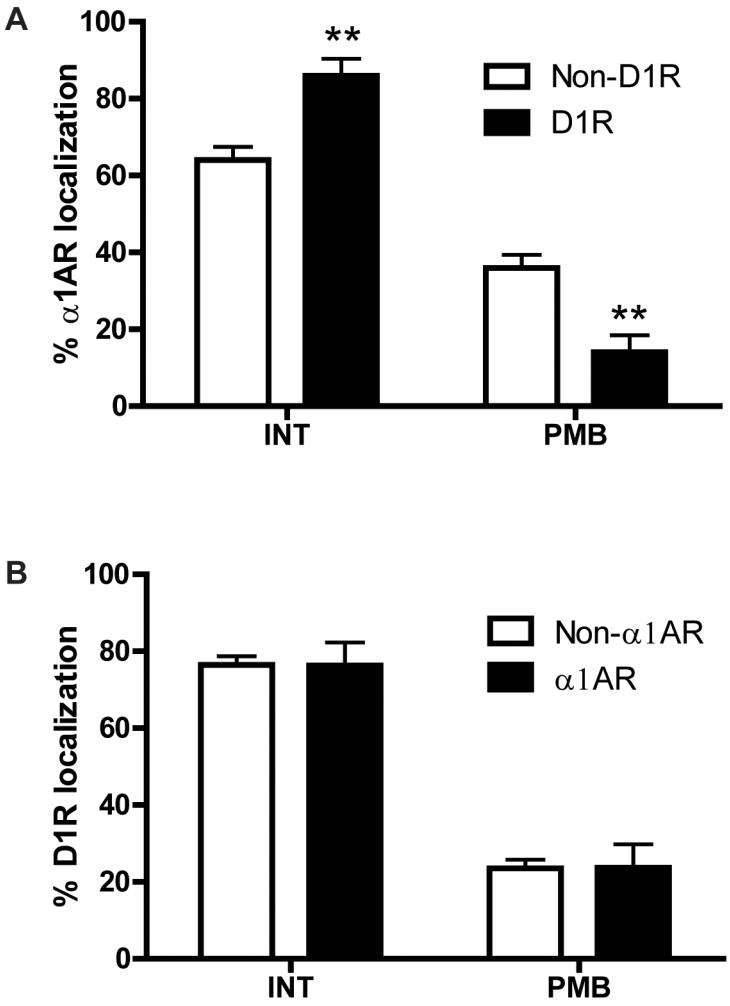

Fig. 4. Subcellular localization of D1R and α1AR in single and double labeled PFC dendrites

(A) Mean ± SEM percent of intracellular (INT) and plasma membrane bound (PMB) α1AR immunogold particles in dendrites that contain (D1R) or do not contain (non-D1R) D1R immunoperoxidase labeling. Total number of labeled elements examined: 63 D1R-positive dendrites, 26 D1R-negative dendrites. (B) Mean ± SEM percent of INT and PMB D1R immunogold particles in dendrites that contain (α1AR) or do not contain (non-α1AR) α1AR immunoperoxidase labeling. Total number of labeled elements examined: 89 α1AR-positive dendrites, 58 α1AR-negative dendrites. **p<0.01 compared with non-D1R for that location. N=4 rats.

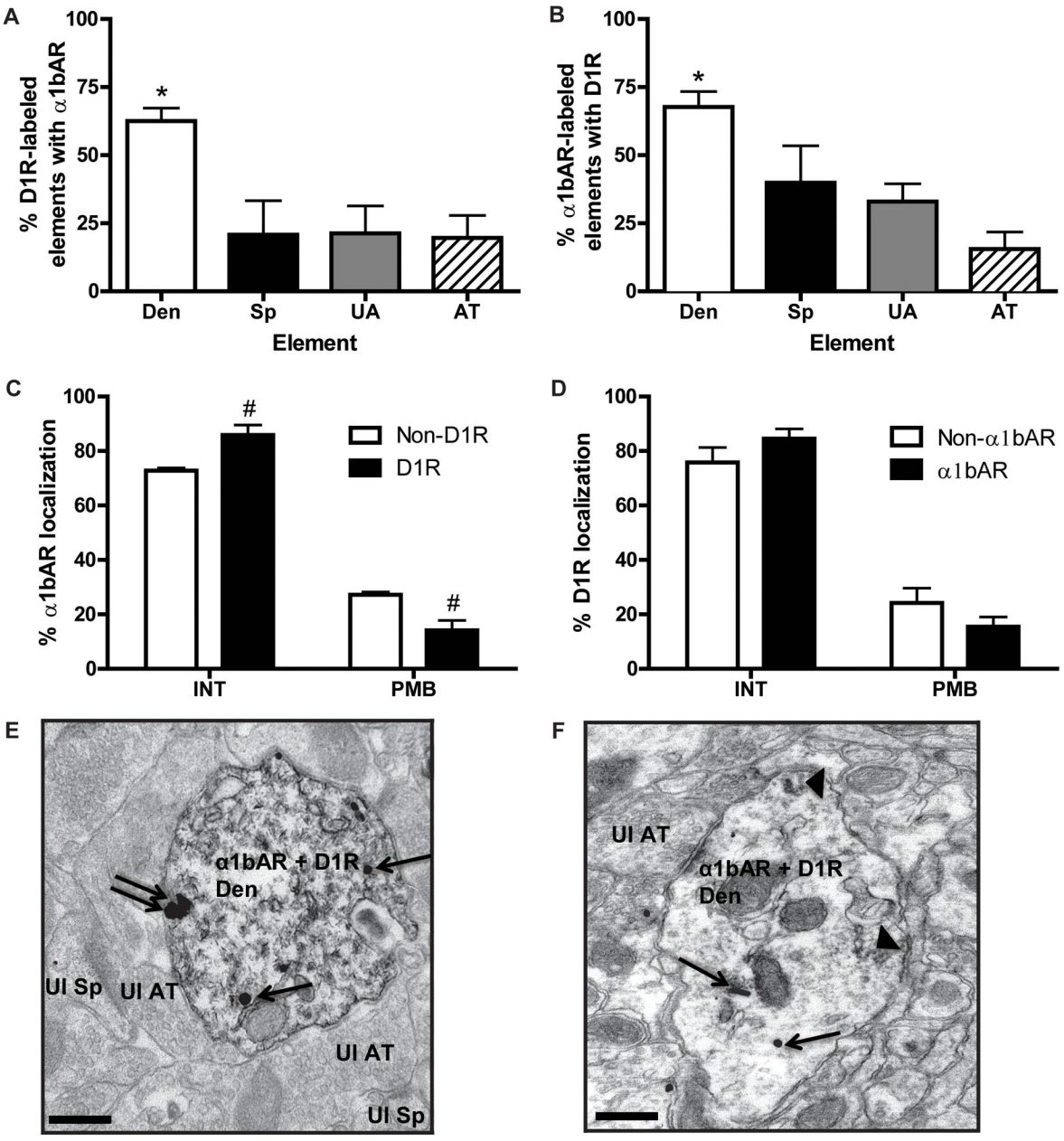

Fig. 5. Co-localization and distribution of D1R and α1bAR in the PFC

(A) Mean ± SEM percent of D1R immunoperoxidase-labeled elements that also contain α1bAR immunogold labeling. N=4 rats. Total number of D1R-labeled elements examined: 91 dendrites, 12 spines, 35 unmyelinated axons, 38 axon terminals. *p<0.05 compared to each other type of element. (B) Mean ± SEM percent of α1bAR immunoperoxidase-labeled elements that also contain D1R immunogold labeling. N=5 rats. Total number of α1bAR labeled elements examined: 211 dendrites, 43 spines, 166 unmyelinated axons, and 89 axon terminals. *p<0.05 compared to each other type of element. (C) Mean ± SEM percent of INT and PMB α1bAR immunogold particles in dendrites that contain (D1R) or do not contain (non-D1R) D1R immunoperoxidase labeling. #p<0.05 compared to non-D1R for that location. (D) Mean ± SEM percent of INT and PMB D1R immunogold particles in dendrites that contain (α1bAR) or do not contain (non-α1bAR) α1bAR immunoreactivity.

(E) Representative electron micrograph of a double labeled dendrite (Den) for D1R (immunoperoxidase, diffuse throughout) and α1bAR (immunogold). An unlabeled spine (Ul Sp) and axon terminal (Ul AT) are also indicated. (F) Representative micrograph of a dendrite with α1bAR immunoperoxidase labeling (arrowheads) and D1R immunogold labeling. For (E) and (F), single arrows indicate intracellular immunogold labeling, while double arrows indicate extrasynaptic plasma membrane bound labeling. Scale bars = 0.5 μm.

Table 1

Antigens	Immunogen	Manufacturer Data	Dilution Used
α1AR	Synthetic peptide corresponding to residues K(339)FSREKKA KT(349) of 3rd intracellular loop of human α 1AR.	Thermo Scientific, Pierce Antibodies, Rabbit Polyclonal, #PA1-047	1:1000
α1bAR	15 amino acid peptide from the C-terminal residues of human α1bAR.	Abcam, Rabbit Polyclonal, #ab84405	1:3000
D1R	Recombinant fusion protein containing the C-terminal 97 amino acids of human D1 receptor.	Sigma-Aldrich, Rat, Monoclonal, #D2944	1:500